

GAP SOLITONS FOR THE REPULSIVE GROSS-PITAEVSKII EQUATION WITH PERIODIC POTENTIAL: CODING AND METHOD FOR COMPUTATION

GEORGY L. ALFIMOV, PAVEL P. KIZIN

Moscow Institute of Electronic Engineering, Zelenograd, Moscow, 124498, Russia

DMITRY A. ZEZYULIN

Centro de Física Teórica e Computacional and Departamento de Física,
Faculdade de Ciências da Universidade de Lisboa, Campo Grande, Ed. C8, Lisboa P-1749-016, Portugal

(Communicated by the associate editor name)

ABSTRACT. The paper is devoted to nonlinear localized modes (“gap solitons”) for the spatially one-dimensional Gross-Pitaevskii equation (1D GPE) with a periodic potential and repulsive interparticle interactions. It has been recently shown (G. L. Alfimov, A. I. Avramenko, *Physica D*, 254, 29 (2013)) that under certain conditions all the stationary modes for the 1D GPE can be coded by bi-infinite sequences of symbols of some finite alphabet (called “codes” of the solutions). We present and justify a numerical method which allows to reconstruct the profile of a localized mode by its code. As an example, the method is applied to compute the profiles of gap solitons for 1D GPE with a cosine potential.

1. Introduction. The Gross–Pitaevskii equation (GPE) is a commonly recognized model for description of nonlinear matter waves in Bose–Einstein condensates (BECs) [20]. In the dimensionless form spatially one-dimensional (1D) GPE,

$$i\Psi_t = -\Psi_{xx} + U(x)\Psi + \sigma|\Psi|^2\Psi, \quad \sigma = \pm 1, \quad (1)$$

describes the dynamics of a cigar-shaped BEC cloud in the so-called mean-field approximation. In (1) the variables are properly scaled, $\Psi = \Psi(t, x)$ is the complex-valued macroscopic wavefunction of the condensate, and its squared amplitude $|\Psi(t, x)|^2$ describes the local density of BEC. The nonlinear term $\sigma|\Psi|^2\Psi$ takes into account the interactions between the particles: the case $\sigma = 1$ corresponds to the repulsive interparticle interactions, $\sigma = -1$ corresponds to the attractive interactions. Both these cases are of physical relevance. The real-valued potential $U(x)$ describes a trap which confines the BEC. In the case of optical confinement of BEC, the potential $U(x)$ is a periodic function.

An important particular class of solutions of the GPE corresponds to the stationary modes. These modes are of the form $\Psi(t, x) = e^{-i\omega t}\psi(x)$ and the wavefunction $\psi(x)$ solves the stationary GPE

$$\psi_{xx} + (\omega - U(x))\psi - \sigma|\psi|^2\psi = 0. \quad (2)$$

2010 *Mathematics Subject Classification.* 35Q55, 35C08, 34C41, 37B10, 65P99.

Key words and phrases. Gross-Pitaevskii equation, gap solitons, nonlinear modes, coding.

The third author is supported by FCT (Portugal) through the grant No. UID/FIS/00618/2013.

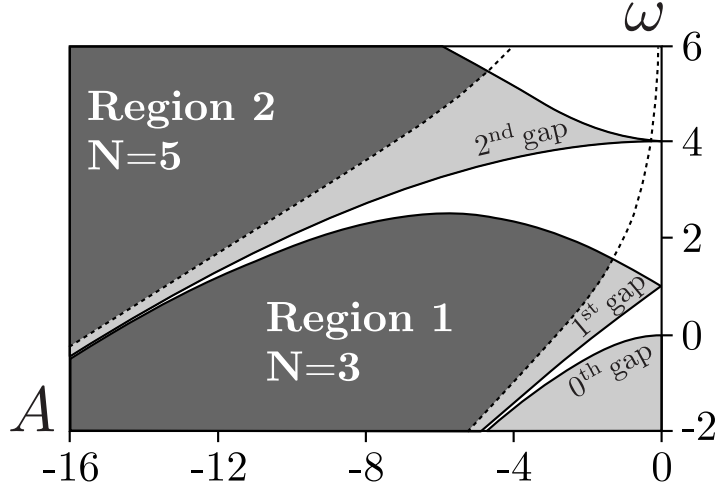


FIGURE 1. The diagram of gaps and bands of the Matheiu equation $\psi_{xx} + (\omega - A \cos 2x)\psi = 0$. The regions where according to [3] the coding of bounded solutions for the nonlinear equation (4) is possible are shown in the first and the second gaps: if ω and A belong to Region 1, then the bounded solutions can be coded using an alphabet of $N = 3$ symbols; in Region 2 an alphabet of $N = 5$ symbols is necessary.

The stationary modes of the condensate that satisfy the localization conditions

$$\lim_{x \rightarrow \pm\infty} \psi(x) = 0 \quad (3)$$

can be regarded as *real-valued* [2] and satisfying the 1D real stationary GPE

$$\psi_{xx} + (\omega - U(x))\psi - \sigma\psi^3 = 0, \quad \psi, x \in \mathbb{R}. \quad (4)$$

If the potential $U(x)$ is periodic, the modes satisfying (3) and (4) are called *gap solitons*. This terminology can be understood if one considers the linear version of (4), i.e.

$$\psi_{xx} + (\omega - U(x))\psi = 0. \quad (5)$$

Due to the conditions (3), (5) approximates (4) for $|x| \gg 1$. Equation (5) is a linear eigenvalue problem for the Schrödinger operator with periodic potential $U(x)$ and eigenvalue ω . It is well-known [11], that the spectrum of such a problem typically consists of a countable set of continuous *bands* separated by *gaps*. Zero boundary conditions at $x \rightarrow +\infty$ and $x \rightarrow -\infty$ for (5) cannot be satisfied if ω lies in a band of the spectrum. Therefore the solutions of (4) satisfying (3) can exist only if ω belongs to one of the gaps.

It is known that apart from the gap solitons [2, 15, 16, 19], (4) supports nonlinear periodic structures (nonlinear Bloch waves) [16, 21], domain walls [13], gap waves [1] and so on. The authors of [23, 24] observed that more complex structures described by (4), such as nonlinear Bloch waves, can be built from elementary entities called *fundamental gap solitons* (FGS) by means of the so-called *composition relation*. This idea was further developed in [3], where it was suggested to code complex nonlinear modes of (4) using the methods of symbolic dynamics. The approach of [3] is consistent with the recent results of [12] where it was proved that in the

semiclassical limit a certain class of gap solitons for (4) can be mapped to a set of localized modes of Discrete Nonlinear Schrödinger Equation (DNLS) which admit the description in terms of coding sequences [4].

The “coding” approach of [3] exploits the following fact. In the case of repulsive interactions ($\sigma = 1$) the “most” of the solutions of (4) *collapse* (i.e., tend to infinity) at some finite point of the real axis. The complementary set of non-collapsing solutions (including all gap soliton solutions) can be associated with a set on the plane of initial conditions for (4). This set has fractal structure and under certain conditions (Hypotheses 1-3 of [3]) it can be described in terms of symbolic dynamics and mapped into the set of bi-infinite sequences of symbols of some finite alphabet \mathcal{A} . The relation between the solutions and the codes is a homeomorphism: each bounded in \mathbb{R} solution of (4) corresponds to unique bi-infinite code of the type

$$\{\dots, i_{-1}, i_0, i_1, \dots\}, \quad i_k \in \mathcal{A},$$

and each code of this type corresponds to unique bounded in \mathbb{R} solution of (4). It was argued in [3], that in the case of the cosine potential

$$U(x) = A \cos 2x \tag{6}$$

this coding is possible for vast areas in the parameter plane (ω, A) . These areas are situated in the gaps of linear equation (5) which becomes the Mathieu equation for the cosine potential (6) (see Figure 1). For Region 1 (situated in the first gap), the alphabet \mathcal{A} consists of three symbols, while in the Region 2 (situated in the second gap of the Mathieu equation) the alphabet of five symbols must be used.

In order to transform the coding approach into a convenient tool for analysis and computation of gap solitons, one has to answer the following practical questions:

QUESTION 1. How can one get a code of a given gap soliton?

QUESTION 2. How can one compute a profile of gap soliton by its code?

The answer to the Question 1 is relatively simple (see subsection 4.1) and follows immediately from the results of [3]. The answer to the Question 2 is not simple, and it is the focal point of this paper. From the practical point of view, the answer to this question offers a method for numerical computation of gap solitons. While several numerical approaches to this task have been described in the literature (see, for instance, a survey in the monograph [22]), the peculiar advantage of a coding-based numerical algorithm is that it yields a nonlinear mode which corresponds to the specific code chosen beforehand. Applying the algorithm to different codes it is possible to compute and classify gap solitons with shapes of different complexity assigned in advance.

Looking ahead, we note that a high-accuracy algorithm for computation of nonlinear modes is a crucial ingredient of the numerically accurate stability analysis. It is known that even the simplest FGSs from lower gaps undergo oscillatory instabilities under both attractive [19] and repulsive [14] nonlinearities (instabilities of this type have been also found in the coupled mode limit [9, 10, 17]). The oscillatory instabilities of gap solitons can be extremely weak and can be revealed by a quite thorough study only [14]. This, in particular, requires to compute the profile of nonlinear mode with high accuracy.

In what follows, the consideration is restricted by the repulsive version of GPE ($\sigma = 1$). Section 2 contains a brief description of the coding approach. Section 3 includes some theoretical results necessary for construction of the algorithm. Section 4 contains the description of the main numerical algorithm whose listing is

presented in Appendix B. In section 5, the method is illustrated for the GPE with cosine potential (6). Section 6 concludes the paper and presents a short outlook for the future work.

2. Review of the coding approach. Let us briefly describe the method for coding of nonlinear modes for (4) (see [3] for the detailed presentation). The basis of this method, the coding theorem, is formulated in subsection 2.3. In order to formulate the coding theorem, in subsection 2.1 and 2.2 we introduce several definitions, assumptions, and auxiliary concepts.

2.1. Collapsing solutions. For $\sigma = 1$ the equation (4) for the nonlinear modes reads

$$\psi_{xx} + (\omega - U(x))\psi - \psi^3 = 0, \quad \psi, x \in \mathbb{R}. \quad (7)$$

The potential $U(x)$ is assumed to be bounded, π -periodic and even. A prototypical example is the cosine potential (6). The following definitions are necessary, [3].

Definition 2.1. The solution $\psi(x)$ of Cauchy problem $\psi(0) = \psi_0$, $\psi_x(0) = \psi'_0$ of (7) collapses to $+\infty$ (respectively, collapses to $-\infty$) at the point $x = x_0 > 0$ if $\lim_{x \rightarrow x_0-0} \psi(x) = +\infty$, (respectively, $\lim_{x \rightarrow x_0-0} \psi(x) = -\infty$). Similarly, the solution $\psi(x)$ of this Cauchy problem collapses to $+\infty$ (respectively, collapses to $-\infty$) at the point $x = x_0 < 0$ if $\lim_{x \rightarrow x_0+0} \psi(x) = +\infty$ (respectively, $\lim_{x \rightarrow x_0+0} \psi(x) = -\infty$).

The balance of dispersive and nonlinear terms in (7) allows to conclude that in vicinity of singularity $x = x_0$ the asymptotics of a collapsing solution is

$$\psi(x) \sim \pm \frac{\sqrt{2}}{x - x_0}.$$

Definition 2.2. Let (ψ_0, ψ'_0) be a point on the plane $\mathbb{R}^2 = (\psi, \psi')$. Let $\psi(x)$ be a solution of the Cauchy problem for (7) with inital data $\psi(0) = \psi_0$, $\psi_x(0) = \psi'_0$. Then the point (ψ_0, ψ'_0) is called

- P -collapsing to $+\infty$ (or $-\infty$), if the solution $\psi(x)$ collapses to $+\infty$ (correspondingly, to $-\infty$) at the point $x = P$;
- P -non-collapsing forward point, if $\psi(x)$ does not collapse at any $x \in (0; P]$;
- P -non-collapsing backward point, if $\psi(x)$ does not collapse at any $x \in [-P; 0)$.

Example. Let $U(x) \equiv 0$ and $\omega = 0$. Then:

- a. The solution of Cauchy problem for (7) and $\psi(0) = \psi_x(0) = \sqrt{2}$ is

$$\psi(x) = \frac{\sqrt{2}}{1 - x}.$$

Then $\psi(x)$ collapses to $+\infty$ at $x_0 = 1$. The point $(\sqrt{2}, \sqrt{2})$ is 1-collapsing to $+\infty$ point. Simultaneously, it is ∞ -non-collapsing backward point, since no collapse occurs at the interval $(-\infty; 0)$.

- b. The solution of Cauchy problem for (7) and $\psi(0) = 1$, $\psi_x(0) = 0$ is

$$\psi(x) = \frac{1}{\text{cn}(x; \sqrt{2}/2)}.$$

Here $\text{cn}(x; k)$ is the Jacobi elliptic function. Then $\psi(x)$ collapses to $+\infty$ at $x_{\pm} = \pm K(\sqrt{2}/2)$, where $K(\xi)$ is the complete elliptic integral of the first kind. The point $(1, 0)$ is $K(\sqrt{2}/2)$ -collapsing to $+\infty$ point and $-K(\sqrt{2}/2)$ -collapsing to $+\infty$ point.

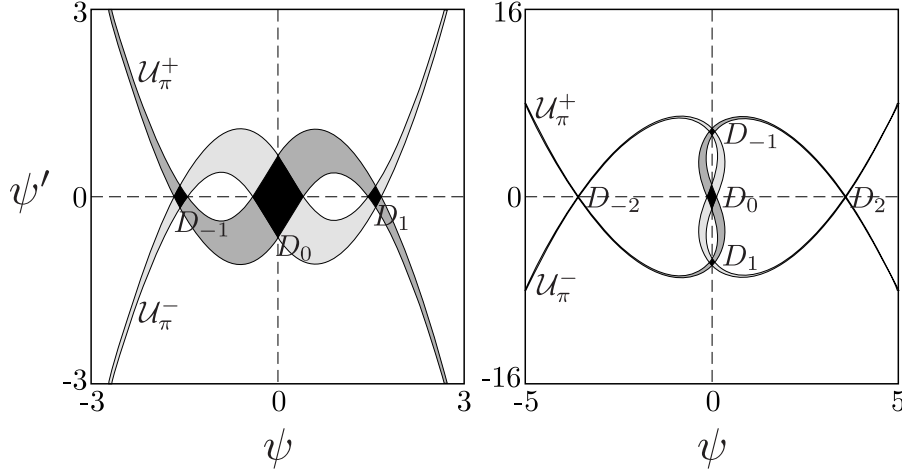


FIGURE 2. The sets \mathcal{U}_π^\pm and Δ_0 for (7) with the potential (6). Panel (a): parametric point $(\omega, A) = (1, -3)$ from Region 1 in Figure 1, in this case Δ_0 consists of three connected components, D_{-1} , D_0 and D_1 ; Panel (b): parametric point $(\omega, A) = (4, -10)$ from Region 2 in Figure 1, in this case Δ_0 consists of five connected components, from D_{-2} to D_2 .

Also, since $K(\sqrt{2}/2) \approx 1.854 > 1$ one can say that the point $(1, 0)$ is 1-non-collapsing forward point and 1-non-collapsing backward point.

Definition 2.3. For (7) denote by \mathcal{U}_P^+ the set of all P -non-collapsing forward points and by \mathcal{U}_P^- the set of all P -non-collapsing backward points.

Definition 2.4. Define the Poincare map $T : \mathbb{R}^2 \rightarrow \mathbb{R}^2$ associated with (7) as follows: for a point $(\psi_0, \psi'_0) \in \mathbb{R}^2$, $T(\psi_0, \psi'_0) = (\psi(\pi), \psi_x(\pi))$ where $\psi(x)$ is a solution of the Cauchy problem for (7) with initial data $\psi(0) = \psi_0$ and $\psi_x(0) = \psi'_0$.

The Poincare map T and the sets \mathcal{U}_π^\pm for (7) have the following properties:

1. T is an area-preserving diffeomorphism.
2. T is defined on the set \mathcal{U}_π^+ only. Correspondingly, inverse map T^{-1} is defined on the set \mathcal{U}_π^- . Moreover, $T\mathcal{U}_\pi^+ = \mathcal{U}_\pi^-$ and $T^{-1}\mathcal{U}_\pi^- = \mathcal{U}_\pi^+$.
3. Since $U(x)$ is an even function, the sets \mathcal{U}_π^\pm are symmetric with respect to ψ .
4. Since the nonlinearity in (7) is an odd function of ψ , the sets \mathcal{U}_π^\pm are symmetric with respect to the origin $(0, 0)$.
5. Since \mathcal{U}_π^\pm are symmetric with respect to ψ and $(0, 0)$, they are symmetric with respect to ψ' .
6. The boundary of \mathcal{U}_π^+ (to be denoted by $\partial\mathcal{U}_\pi^+$) consists of π -collapsing to $+\infty$ or $-\infty$ points. This boundary is formed by continuous curves (Corollary of Theorem 2.2 in [3], see also [6]) and is symmetric with respect to the origin. Moreover, if some point (ψ, ψ') of $\partial\mathcal{U}_\pi^+$ is π -collapsing to $+\infty$, then the symmetric point $(-\psi, -\psi')$ also belongs to $\partial\mathcal{U}_\pi^+$ and it is π -collapsing to $-\infty$. The similar situation takes place for $\partial\mathcal{U}_\pi^-$, the boundary of \mathcal{U}_π^- . It consists of $-\pi$ -collapsing to $+\infty$ of $-\infty$ points.

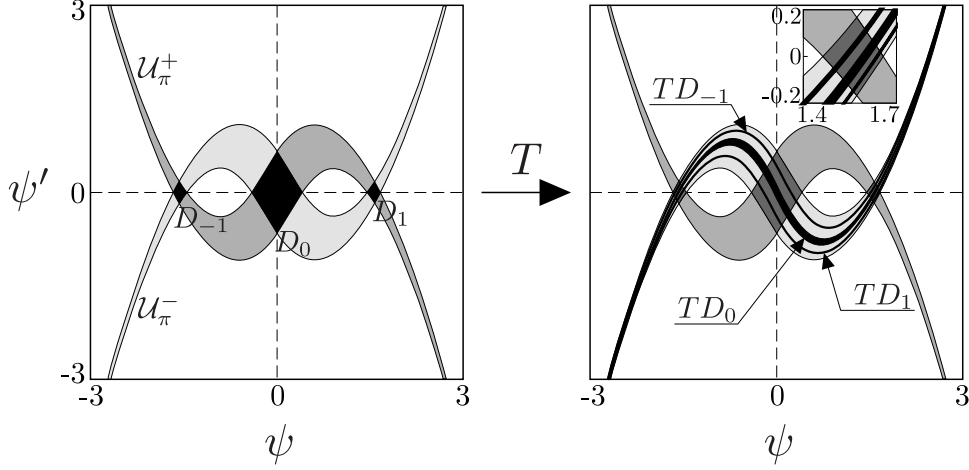


FIGURE 3. Action of the map T on Δ_0 which consists of three connected components, D_{-1} , D_0 and D_1 . The cosine potential (6) was used for (7). Parameters are $\omega = 1$ and $A = -3$.

Definition 2.5. Denote

$$\Delta_0 = \mathcal{U}_\pi^+ \cap \mathcal{U}_\pi^-. \quad (8)$$

Evidently, Δ_0 consists of the points that have both T -image and T -pre-image. The features of Δ_0 are as follows:

1. Δ_0 is bounded (Theorem 2.1 in [3]) and includes the origin $(0, 0)$.
2. Δ_0 is open (it follows from Theorem 2.2 in [3]).
3. If Δ_0 consists of the finite number N of connected components, then N is odd ($N \geq 3$), and for each connected component $D \subset \Delta_0$ and $(0, 0) \notin D$ one can find a dual component $D^* \subset \Delta_0$ such that D and D^* are situated symmetrically with respect to the origin.

Definition 2.6. The sets Δ_n^\pm , $n = 0, 1, \dots$ are defined by the following recurrence rule

$$\Delta_0^- = \Delta_0, \quad \Delta_{n+1}^- = T\Delta_n^- \cap \Delta_0, \quad (9)$$

$$\Delta_0^+ = \Delta_0, \quad \Delta_{n+1}^+ = T^{-1}\Delta_n^+ \cap \Delta_0. \quad (10)$$

Evidently, if $p \in \Delta_n^+$ then there exist $Tp \in \Delta_{n-1}^+ \subseteq \Delta_0$, $T^2p \in \Delta_{n-2}^+ \subseteq \Delta_0$, \dots , $T^n p \in \Delta_0$. On the other hand, if for a point $p \in \Delta_0$ there exists $q = T^n p \in \Delta_0$, then $T^{-1}q = T^{n-1}p \in \Delta_1^+$, $T^{-2}q = T^{n-2}p \in \Delta_2^+$, etc. Repeating the procedure n times one arrives at the relations

$$\begin{aligned} \{p \in \Delta_n^+\} &\iff \{p, Tp, T^2p, \dots, T^n p \in \Delta_0\}, \\ \{p \in \Delta_n^-\} &\iff \{p, T^{-1}p, T^{-2}p, \dots, T^{-n}p \in \Delta_0\}. \end{aligned}$$

These relations imply that

$$\begin{aligned} \dots &\subset \Delta_{n+1}^+ \subset \Delta_n^+ \subset \dots \subset \Delta_1^+ \subset \Delta_0, \\ \dots &\subset \Delta_{n+1}^- \subset \Delta_n^- \subset \dots \subset \Delta_1^- \subset \Delta_0 \end{aligned}$$

Let us illustrate the construction of the sets Δ_n^\pm by an example. Figure 3 shows the action of T on Δ_0 for the case of potential $U(x) = -3 \cos 2x$ and $\omega = 1$. The set

Δ_0 consists of three connected components, marked D_{-1} , D_0 and D_1 . T -images of these components are three infinite strips. Each of these infinite strips intersects each of the connected components $D_{-1,0,1}$, and therefore the set $\Delta_1^- = T\Delta_0 \cap \Delta_0$ consists of nine connected components. Further, the set Δ_2^- consists of 27 connected components and so on. The sets Δ_n^+ are symmetric to Δ_n^- with respect to ψ -axis, so they have the same properties.

2.2. Assumptions. Recall that a function $f(x)$ is called *Lipschitz function* if there exists finite $\varkappa > 0$ such that for any x_1 and x_2 one has $|f(x_2) - f(x_1)| \leq \varkappa|x_2 - x_1|$. In order to formulate the main result of [3] let us introduce the following definitions.

Definition 2.7. Let us call a plane curve γ on the plane (ψ, ψ') increasing (correspondingly, decreasing), if γ is a graph of increasing (correspondingly, decreasing) Lipschitz function $\psi' = G(\psi)$.

Definition 2.8 (An island). We call an island an open curvilinear quadrangle $D \subset \mathbb{R}^2$ bounded by two pairs of curve segments, such that the segments from one pair do not intersect and are increasing, and the segments from another pair do not intersect and are decreasing.

Let us make the following assumptions about the set Δ_0 and the map T associated with (7).

Hypothesis 1. The set Δ_0 defined by (8) consists of $N = 2L + 1$ disjoint islands D_i , $i = -L, \dots, L$.

We say that one boundary of an island is opposite to another boundary if these two boundaries do not intersect.

Hypothesis+. For each island D_i from Hypothesis 1, one boundary of D_i consists of π -collapsing to $+\infty$ points, and the opposite boundary consists of π -collapsing to $-\infty$ points. Similarly, from another pair of opposite boundaries, one consists of $-\pi$ -collapsing to $+\infty$ points, and another consists of $-\pi$ -collapsing to $-\infty$ points.

In what follows, for an island D_i , we will denote α_i^\pm the boundaries consisting of π -collapsing to $\pm\infty$ points and denote β_i^\pm the boundaries consisting of $-\pi$ -collapsing to $\pm\infty$ points, see Figure 4.

Hypothesis+ naturally holds when \mathcal{U}_π^\pm are infinite curvilinear strips (see Figure 2 as an example). In this case the boundary $\partial\mathcal{U}_\pi^+$ is formed by two curves, one of them consists of π -collapsing to $+\infty$ points and other one consists of π -collapsing to $-\infty$ points. These curves can be mapped one into another by reflection with respect to the origin. The similar situation takes place for the boundary $\partial\mathcal{U}_\pi^-$. The opposite sides α^\pm of each island are formed by segments of opposite boundaries of $\partial\mathcal{U}_\pi^+$, as well as opposite sides β^\pm are formed by segments of opposite boundaries of $\partial\mathcal{U}_\pi^-$.

Definition 2.9 (v - and h - curves). Let D be one of the islands from Hypothesis 1 bounded by curve segments α^\pm and β^\pm . We call v -curve a Lipschitz curve β with endpoints on α^- and α^+ which is increasing if β^\pm are increasing and is decreasing if β^\pm are decreasing. Similarly, we call h -curve a Lipschitz curve α with endpoints on β^- and β^+ which is increasing if α^\pm are increasing and is decreasing if α^\pm are decreasing.

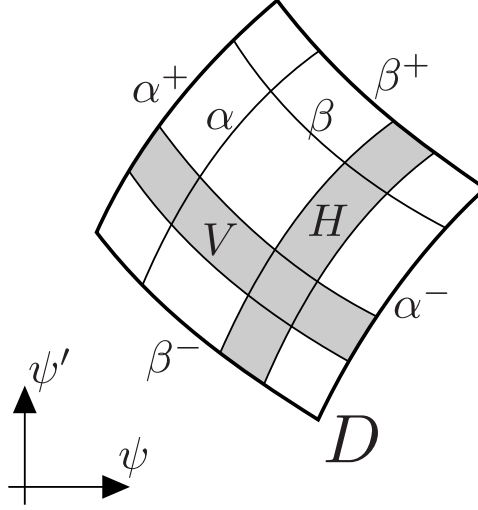


FIGURE 4. An island D with v -curve β , v -strip V , h -curve α and h -strip H .

Definition 2.10 (v - and h - strips). Let D be an island. We call v -strip an open curvilinear strip between two non-intersecting v -curves. Similarly, we call h -strip an open curvilinear strip between two non-intersecting h -curves.

Hypothesis 2. The Poincare map T associated with (7) is such that

- (a) T maps v -strips of any island D_i , $i = -L, \dots, L$ from Δ_0 in such a way that for any v -strip V , $V \subseteq D_i$, each of the intersections $TV \cap D_j$, $j = -L, \dots, L$, is nonempty and is a v -strip.
- (b) T^{-1} maps h -strips of any D_i , $i = -L, \dots, L$, in such a way that for any h -strip H , $H \subseteq D_i$, each of the intersections $T^{-1}H \cap D_j$, $j = -L, \dots, L$, is nonempty and is an h -strip.

Hypothesis 3. The sets Δ_n^\pm defined by (9), (10) are such that

$$\lim_{n \rightarrow \infty} \mu(\Delta_n^\pm) = 0,$$

where $\mu(S)$ is the area of S .

For any particular choice of potential $U(x)$ and parameter ω the validity of Hypotheses 1–3 should be supported by numerical arguments. On the basis of a systematic numerical investigation, the following conjecture was formulated in [3]:

Conjecture. If the parameters ω and A for (7) with the cosine potential (6) belong to dark gray areas (Regions 1 and 2) on the parameter plane (ω, A) in Figure 1, then Hypotheses 1–3 hold.

The upper boundaries of Regions 1 and 2 coincide with upper boundary of the first and the second gap, respectively. The lower boundaries of these regions correspond to breaking of Hypothesis 1: if ω and A lie below these boundaries, then Δ_0 is not split into a set of disjoint islands, i.e., Hypothesis 1 does not hold. Hypothesis+ was not introduced in [3]. However for ω and A lying in Regions 1 and 2 the sets \mathcal{U}_π^\pm are curvilinear strips bounded by two curves, consisting of $\pm\pi$ -collapsing to

$+\infty$ points and of $\pm\pi$ -collapsing to $-\infty$ points correspondingly. This implies that Hypothesis+ also holds for ω and A lying in Regions 1 and 2.

2.3. Coding theorem.

Definition 2.11. Denote by Ω^N , $N = 2L + 1$, the set of bi-infinite sequences $\{\dots, i_{-1}, i_0, i_1, \dots\}$, $i_k = -L, \dots, L$.

The set Ω^N has the structure of a topological space where the neighborhood of a point $a^* = \{\dots, i_{-1}^*, i_0^*, i_1^*, \dots\}$ is defined by the sets

$$W_k(a^*) = \{a \in \Omega^N \mid i_j = i_j^*, |j| < k\}, \quad k = 1, 2, \dots$$

Definition 2.12. Denote by \mathcal{P} the set of bi-infinite sequences (called orbits)

$$\mathbf{s} = \{\dots, p_{-1}, p_0, p_1, \dots\}, \quad Tp_n = p_{n+1},$$

where each $p_n = (\psi_n, \psi'_n)$, $n = 0, \pm 1, \pm 2, \dots$, belongs to Δ_0 .

It is clear that any orbit is uniquely determined by its single entry, for instance, p_0 . The point p_0 cannot be arbitrary since, as it was mentioned before, a great part of points of the plane of initial data are collapsing, either forward or backward (or both), and a collapsing point cannot generate a bi-infinite sequence \mathbf{s} . The set \mathcal{P} has the structure of a metric space where the distance ρ between the elements $\mathbf{s}^{(1)} = \{\dots, p_{-1}^{(1)}, p_0^{(1)}, p_1^{(1)}, \dots\}$ and $\mathbf{s}^{(2)} = \{\dots, p_{-1}^{(2)}, p_0^{(2)}, p_1^{(2)}, \dots\}$ is defined as Euclidean distance between the points $p_0^{(1)}$ and $p_0^{(2)}$ in \mathbb{R}^2 ,

$$\rho(\mathbf{s}^{(1)}, \mathbf{s}^{(2)}) = \sqrt{\left(\psi_0^{(2)} - \psi_0^{(1)}\right)^2 + \left(\psi_0'^{(2)} - \psi_0'^{(1)}\right)^2}.$$

Definition 2.13. Define a map $\Sigma : \mathcal{P} \rightarrow \Omega^N$ as follows: i_k is the number i of the component D_i where the point p_k lies.

The following statement was proved in [3]:

Theorem 2.14. Assume that Hypotheses 1–3 hold. Then Σ is a homeomorphism between the topological spaces \mathcal{P} and Ω^N .

In the rest of the paper we assume that Hypotheses 1–3 and Hypothesis+ hold.

3. Structure of the set Δ_0 . Consider the structure of the set Δ_0 in details. According to the made assumptions, Δ_0 consists of N islands, $N = 2L + 1$, indexed as D_{-L}, \dots, D_L . By Theorem 2.14, there exists a homeomorphism between the set of bi-infinite orbits and “codes” of the form $\{\dots, i_{-1}, i_0, i_1, \dots\}$, where each i_k is a number in the range $-L, -L + 1, \dots, L$. Presence of a number i_k at some position of the code means that at the corresponding T -iteration the orbit visits the island D_{i_k} .

3.1. Indexing of h -strips in an island. Consider the action of the Poincare map T on an island D_i . The points that are sent by T from the island D_i to an island D_j constitute the set $T^{-1}D_j \cap D_i \subseteq \Delta_1^+$. Due to Hypothesis 2, this set is an h -strip. Denote

$$H_{ij} \equiv T^{-1}D_j \cap D_i. \quad (11)$$

By analogy, consider points that visit the islands $D_{i_0}, D_{i_1}, \dots, D_{i_n}$ under the action of T in the given order. Any point p in D_{i_0} whose orbit visits the islands in this

order belongs to an h -strip $H_{i_0 \dots i_n}$ which can be constructed using the following recurrence rule

$$H_{i_k \dots i_n} \equiv T^{-1} H_{i_{k+1} \dots i_n} \cap D_{i_k}. \quad (12)$$

In other words, the h -strip $H_{i_0 \dots i_n}$ coincides with the set of points $p \in \mathbb{R}^2$ satisfying three conditions:

- (a) $p \in D_{i_0}$;
- (b) there exist Tp, T^2p, \dots, T^np ;
- (c) $Tp \in D_{i_1}, T^2p \in D_{i_2}, \dots, T^np \in D_{i_n}$.

The points (a)–(c) imply that the h -strips with different multi-indices are embedded in the following sense

$$\dots \subset H_{i_0 \dots i_n} \subset H_{i_0 \dots i_{n-1}} \subset \dots \subset H_{i_0 i_1 i_2} \subset H_{i_0 i_1} \subset D_{i_0}.$$

If a point $p \in H_{i_0 \dots i_n}$ generates an orbit, then this orbit contains a block

$$\{\dots, \underbrace{i_0, i_1, \dots, i_n, \dots}\}.$$

By definition, h -strip $H_{i_0 \dots i_n}$ is bounded by two h -curves. Points from one of them are $(n+1)\pi$ -collapsing to $+\infty$. Denote this h -curve by $\alpha_{i_0 \dots i_n}^+$. By construction, $T^n \alpha_{i_0 \dots i_n}^+ \subset \alpha_{i_n}^+$. Points from another h -curve are $(n+1)\pi$ -collapsing to $-\infty$. Denote this h -curve by $\alpha_{i_0 \dots i_n}^-$ and note that $T^n \alpha_{i_0 \dots i_n}^- \subset \alpha_{i_n}^-$.

The indexing of v -strips is introduced in a similar manner. The points that are sent by T^{-1} from an island D_i to an island D_j constitute a v -strip denoted as

$$V_{ji} \equiv TD_j \cap D_i. \quad (13)$$

By analogy, v -strip denoted as $V_{i_{-n} \dots i_0}$ is the set of points which belong to D_{i_0} and under the action of T^{-1} visited the islands $D_{i_0}, D_{i_{-1}}, \dots, D_{i_{-n}}$ in the given order. This v -strip can be constructed using the recurrence rule

$$V_{i_{-n} \dots i_{-k}} \equiv TV_{i_{-n} \dots i_{-k-1}} \cap D_{i_{-k}}. \quad (14)$$

The v -strips with different multi-indices are embedded according to the following rule

$$\dots \subset V_{i_{-n} \dots i_0} \subset V_{i_{-n+1} \dots i_0} \subset \dots \subset V_{i_{-2} i_{-1} i_0} \subset V_{i_{-1} i_0} \subset D_{i_0}.$$

If a point $p \in V_{i_{-n} \dots i_0}$ generates an orbit, then this orbit contains a block

$$\{\dots, \underbrace{i_{-n}, i_{-n+1}, \dots, i_0, \dots}\}.$$

3.2. The fixed points of T and their stable and unstable manifolds. The following statement is valid.

Theorem 3.1. (a) Each island D_{i^*} contains one and only one fixed point \mathcal{O}_{i^*} of T , corresponding to the code

$$\{\dots, i^*, i^*, i^*, \dots\}.$$

(b) The fixed point \mathcal{O}_{i^*} possesses local unstable manifold \mathcal{V}_{i^*} and local stable manifold \mathcal{H}_{i^*} of T . The local unstable manifold \mathcal{V}_{i^*} is a v -curve and

$$\{p \in \mathcal{V}_{i^*}\} \iff \{T^{-n}p \in D_{i^*} \text{ for } n = 0, 1, \dots, \text{ and } \lim_{n \rightarrow \infty} T^{-n}p = \mathcal{O}_{i^*}\}. \quad (15)$$

The local stable manifold \mathcal{H}_{i^*} is an h -curve and

$$\{p \in \mathcal{H}_{i^*}\} \iff \{T^n p \in D_{i^*} \text{ for } n = 0, 1, \dots, \text{ and } \lim_{n \rightarrow \infty} T^n p = \mathcal{O}_{i^*}\}. \quad (16)$$

(c) The code $\{\dots, i^*, i^*, i_1, i_2, \dots\}$, $i_1 \neq i^*$, corresponds to an orbit $\{\dots, p_{-1}, p_0, p_1, \dots\}$, such that $\lim_{n \rightarrow \infty} p_{-n} = \mathcal{O}_{i^*}$, whereas the code $\{\dots, i_1, i_2, i^*, i^*, \dots\}$, $i_2 \neq i^*$, corresponds to an orbit $\{\dots, p_{-1}, p_0, p_1, \dots\}$, such that $\lim_{n \rightarrow \infty} p_n = \mathcal{O}_{i^*}$.

The proof of Theorem 3.1 is postponed to Appendix A.

The origin $(0, 0)$ is a fixed point of T , and it belongs to one of the islands. It is convenient to enumerate the islands in such a way that the origin belongs to D_0 , i.e., $\mathcal{O}_0 = (0, 0) \in D_0$.

Corollary 1. *The codes*

$$\{\dots, 0, 0, i_1, i_2, \dots, i_m, 0, 0, \dots\}$$

correspond to homoclinic loops of $\mathcal{O}_0 = (0, 0)$.

Remark 1. Since (7) is invariant with respect to the change $\psi(x) \rightarrow -\psi(x)$, the v -curve \mathcal{V}_0 and h -curve \mathcal{H}_0 are symmetric with respect to the origin.

Remark 2. Let $DT(\mathcal{O}_{i^*})$ be the operator of linearization for T at fixed point $\mathcal{O}_{i^*} \in D_{i^*}$. Assume that the eigenvalues λ_1 and λ_2 of $DT(\mathcal{O}_{i^*})$ are such that $\lambda_{1,2}^n \neq 1$, $n = 1, 2, 3, 4$ (see [8], Addition 8). Since T is an area-preserving map, $\lambda_1 \lambda_2 = 1$. Then, due to existence of local stable and unstable manifolds, \mathcal{H}_{i^*} and \mathcal{V}_{i^*} , the fixed point \mathcal{O}_{i^*} is of hyperbolic type. Assume that $|\lambda_1| > 1$, $|\lambda_2| < 1$. If the corresponding eigenvectors of λ_1 and λ_2 are denoted by e_1 and e_2 , then the tangent vector to \mathcal{V}_{i^*} is e_1 and the tangent vector to \mathcal{H}_{i^*} is e_2 .

3.3. Ordering of islands in Δ_0 . In the previous discussion, we used subscripts $i = 0, \pm 1, \dots, \pm L$ to label islands D_i in Δ_0 . It was convenient to assume that the island containing the origin corresponds to $i = 0$, but we have never specified the enumeration of other islands. Let us now fix the ordering of the islands using the following concepts.

Definition 3.2. A curve γ is called an ∞ -curve if $\gamma = T\beta$ where $\beta \subset D$ is a v -curve and D is an arbitrary island.

Lemma 3.3. *An ∞ -curve is a plane Jordan curve without self-intersections, $\gamma = \{(\psi(\xi), \psi'(\xi)), \xi \in (0; 1)\}$, such that $\lim_{\xi \rightarrow 0} \psi(\xi) = -\infty$, $\lim_{\xi \rightarrow 1} \psi(\xi) = +\infty$.*

Proof. By definition, $\gamma = T\beta$ and β is a v -curve. The endpoints of β , b^- and b^+ , are situated on α_i^- and α_i^+ , respectively. Introduce on β a parametrization $q(\xi) = (\psi(\xi), \psi'(\xi))$, $\xi \in (0; 1)$ in such a way that $b^- = q(0)$, $b^+ = q(1)$. The image $T\beta$ is a continuous curve without self-intersection that by Hypothesis 2 crosses each of the islands D_j , $j = -L, \dots, L$, and each intersection $T\beta \cap D_j$ is a v -curve. Moreover, by Hypothesis+ the points $q(0)$ and $q(1)$ are π -collapsing points, $q(0)$ collapses to $-\infty$ and $q(1)$ collapses to $+\infty$. This implies the statement of Lemma 3.3. \square

Corollary 2. TV_i for any $i = -L, \dots, L$ are ∞ -curves. Moreover, $\mathcal{V}_i = TV_i \cap D_i$.

Definition 3.4. Let $\gamma = \{q(\xi), \xi \in (0; 1)\}$ be an ∞ -curve. For two points $q_1 = q(\xi_1) \in \gamma$, $q_2 = q(\xi_2) \in \gamma$ we say that $q_2 \succ q_1$ (or $q_1 \prec q_2$) if $\xi_1 < \xi_2$.

Each ∞ -curve passes through each island exactly once. Let us introduce the order of island with respect to an ∞ -curve.

Definition 3.5. Let $\gamma = \{q(\xi), \xi \in (0; 1)\}$ be an ∞ -curve and D_A and D_B be islands. Let $\gamma \cap D_A$ be v -curve $\{q(\xi), \xi \in (\xi_A^-, \xi_A^+)\}$ and $\gamma \cap D_B$ be v -curve $\{q(\xi), \xi \in (\xi_B^-, \xi_B^+)\}$. We say that $D_B \succ D_A$ (or $D_A \prec D_B$) if $\xi_A^+ < \xi_B^-$.

The following lemma is valid.

Lemma 3.6. *All ∞ -curves pass through the islands in Δ_0 in the same order.*

Proof. We outline the proof as follows. First of all, let us observe that by simple geometric reasons, if two ∞ -curves $\gamma_1 = T\beta^{(1)}$ and $\gamma_2 = T\beta^{(2)}$ ($\beta^{(1)}$ and $\beta^{(2)}$ are v -curves) do not intersect they pass the islands in the same order. This means that if $\beta^{(1)}$ and $\beta^{(2)}$ do not intersect then the statement of the lemma holds. If $\beta^{(1)}$ and $\beta^{(2)}$ intersect they belong to the same island D_{i^*} . Then in D_{i^*} there exists one more v -curve $\beta^{(3)}$ that intersects neither $\beta^{(1)}$ nor $\beta^{(2)}$. By transitivity, one concludes that the statement of the lemma holds for all ∞ -curves. \square

Due to Lemma 3.6, we can use an arbitrary ∞ -curve to order the islands. Consider the ordering of island with respect to ∞ -curve $T\mathcal{V}_0$. Since $T\mathcal{V}_0$ is symmetric with respect to the origin, the origin $(0,0)$ belongs to the “central” island D_0 , and the islands D_i and D_{-i} , $i = 1, 2, \dots, L$ are situated symmetrically with respect to the origin. Let us enumerate the islands according to the introduced order. So in what follows we assume that

$$D_{-L} \prec \dots \prec D_{-1} \prec D_0 \prec D_1 \prec \dots \prec D_L. \quad (17)$$

Definition 3.7. Let γ be an ∞ -curve. Denote

$$h_i^\pm(\gamma) \equiv \gamma \cap \alpha_i^\pm.$$

Remark 3. By construction, the points $h_i^\pm(\gamma)$ are π -collapsing to $\pm\infty$ points.

Remark 4. By simple geometric arguments, one can prove that if $h_i^-(\gamma) \prec h_i^+(\gamma)$ for some ∞ -curve γ , then the same relation $h_i^-(\gamma_1) \prec h_i^+(\gamma_1)$ holds for any other ∞ -curve γ_1 ; vice versa if $h_i^+(\gamma) \prec h_i^-(\gamma)$ for some ∞ -curve γ , then the same relation holds for any other ∞ -curve.

Remark 5. One can also prove that for any two successive islands D_i and D_{i+1} in (17) and for arbitrary ∞ -curve γ one of the two alternatives holds:

$$h_i^-(\gamma) \prec h_i^+(\gamma) \prec h_{i+1}^+(\gamma) \prec h_{i+1}^-(\gamma) \quad \text{or} \quad h_i^+(\gamma) \prec h_i^-(\gamma) \prec h_{i+1}^-(\gamma) \prec h_{i+1}^+(\gamma).$$

Remark 6. In simple terms, if \mathcal{U}_π^+ and \mathcal{U}_π^- are curvilinear strips (as in Figure 2), then the ∞ -curves pass “along” the strip \mathcal{U}_π^- , and the order (17) is the order in which the islands appear in \mathcal{U}_π^- .

3.4. Ordering of h -strips. Consider the h -strip $H_{i_0 \dots i_n} \subset D_{i_0}$ defined in (12). The strip $H_{i_0 \dots i_n}$ contains N non-intersecting h -strips $H_{i_0 \dots i_n i}$, where $i = -L, \dots, L$. Let us address the problem of ordering of $H_{i_0 \dots i_n i}$ within $H_{i_0 \dots i_n}$.

Definition 3.8. Let γ be an ∞ -curve. Denote

$$h_{i_0 \dots i_n}^\pm(\gamma) \equiv \gamma \cap \alpha_{i_0 \dots i_n}^\pm.$$

Definition 3.9. Let $\gamma = \{q(\xi), \xi \in (0; 1)\}$ be an ∞ -curve and H_A and H_B be h -strips. Let $\gamma \cap H_A$ be a segment of curve $\{q(\xi), \xi \in (\xi_A^-, \xi_A^+)\}$ and $\gamma \cap H_B$ be a segment of curve $\{q(\xi), \xi \in (\xi_B^-, \xi_B^+)\}$. We say that $H_B \succ H_A$ (or $H_A \prec H_B$) if $\xi_A^+ < \xi_B^-$.

Theorem 3.10. *Assume that the ordering of islands in Δ_0 is given by (17). Consider the h -strip $H_{i_0 \dots i_n}$ and the embedded h -strips $H_{i_0 \dots i_n i}$, $i = -L, \dots, L$. Then for any ∞ -curve γ the following relations hold*

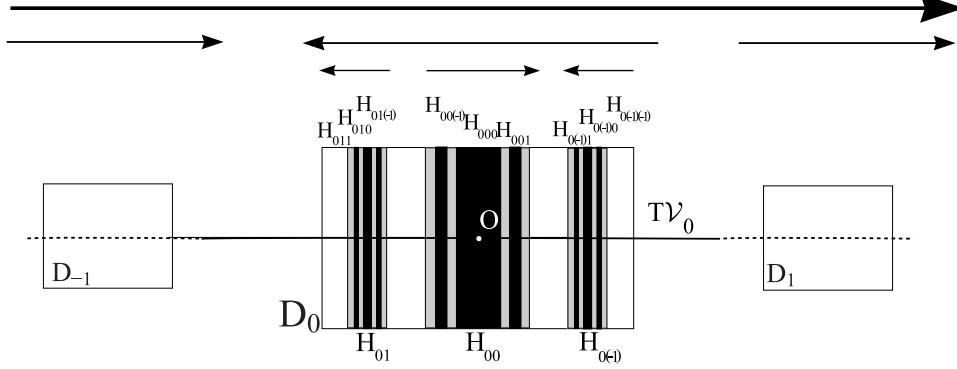


FIGURE 5. Ordering of h -strips in the island D_0 in the case $L = 1$. The island D_0 contains three h -strips with multi-indices of length two: $H_{0(-1)}$, H_{00} , H_{01} . Each of these h -strips contains three h -strips with multi-indices of the length three. Within each of the h -strips the ordering of embedded h -strips inherits the pattern determined by the “global” arrow (in bold) and arrows over each of the islands.

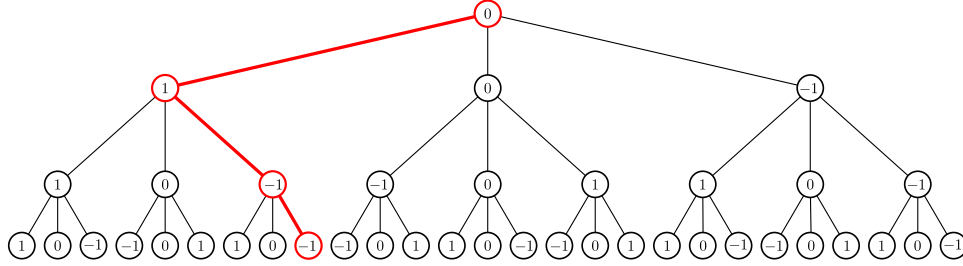


FIGURE 6. The same ordering pattern as in Figure 5 visualized as a ternary tree ($2L + 1 = 3$). As an example, red path (shown by thick lines in the grayscale version of the figure) indicates the position of h -strip $H_{01(-1)(-1)}$. As the graph shows, this h -strip is situated inside $H_{01(-1)}$, to the right from $H_{01(-1)0}$.

- (a) $h_{i_0 \dots i_n}^-(\gamma) \prec h_{i_0 \dots i_n}^+(\gamma) \implies H_{i_0 \dots i_n(-L)} \prec H_{i_0 \dots i_n(-L+1)} \prec \dots \prec H_{i_0 \dots i_n(L)}$
(b) $h_{i_0 \dots i_n}^+(\gamma) \prec h_{i_0 \dots i_n}^-(\gamma) \implies H_{i_0 \dots i_n(L)} \prec H_{i_0 \dots i_n(L-1)} \prec \dots \prec H_{i_0 \dots i_n(-L)}$

Proof. We outline the proof (by induction) as follows. First, we establish the order of h -strips $H_{i_0(-L)}$, $H_{i_0(-L+1)}$, \dots , $H_{i_0(L)}$ within the island D_{i_0} depending on the situation (a) or (b), (the base of induction). Then, by applying the map T it is straightforward to establish the ordering of $H_{i_0 \dots i_{n+1}(-L)}$, $H_{i_0 \dots i_{n+1}(-L+1)}$, \dots , $H_{i_0 \dots i_{n+1}(L)}$ within $H_{i_0 \dots i_{n+1}}$ if the order of $H_{i_0 \dots i_n(-L)}, \dots, H_{i_0 \dots i_n(L)}$ is known (the step of induction). \square

Remark 7. It is also straightforward to prove that if Hypotheses 1–3 and Hypothesis+ hold and the ordering of islands in Δ_0 is given by (17) then the following implications are valid

- (a) $h_{-L}^-(\gamma) \prec h_{-L}^+(\gamma)$, $h_{i_0 \dots i_n}^-(\gamma) \prec h_{i_0 \dots i_n}^+(\gamma) \implies h_{i_0 \dots i_n(-L)}^-(\gamma) \prec h_{i_0 \dots i_n(-L)}^+(\gamma)$

- (b) $h_{-L}^-(\gamma) \prec h_{-L}^+(\gamma), h_{i_0 \dots i_n}^+(\gamma) \prec h_{i_0 \dots i_n}^-(\gamma) \Rightarrow h_{i_0 \dots i_n(-L)}^+(\gamma) \prec h_{i_0 \dots i_n(-L)}^-(\gamma)$
- (c) $h_{-L}^+(\gamma) \prec h_{-L}^-(\gamma), h_{i_0 \dots i_n}^-(\gamma) \prec h_{i_0 \dots i_n}^+(\gamma) \Rightarrow h_{i_0 \dots i_n(-L)}^+(\gamma) \prec h_{i_0 \dots i_n(-L)}^-(\gamma)$
- (d) $h_{-L}^+(\gamma) \prec h_{-L}^-(\gamma), h_{i_0 \dots i_n}^+(\gamma) \prec h_{i_0 \dots i_n}^-(\gamma) \Rightarrow h_{i_0 \dots i_n(-L)}^-(\gamma) \prec h_{i_0 \dots i_n(-L)}^+(\gamma)$

Here γ is an arbitrary ∞ -curve. These implications establish the relation between the orientation of boundaries of the leftmost island D_{-L} , the strip $H_{i_0 \dots i_n}$ and the ordering of the strips $H_{i_0 \dots i_n i}$, $i = -L, \dots, L$ within $H_{i_0 \dots i_n}$.

If the order of the islands and the positions of their boundaries α_i^\pm are known (with respect to an arbitrary ∞ -curve), then the established relations are sufficient to describe positions of h -strips with different indexes. The ordering scheme can be sketched as follows. It is necessary to draw the islands $D_{-L}, D_{-L+1}, \dots, D_L$ from the left to the right, to draw the “global” arrow in the same direction (the upper bold arrow in Figure 5). Next, it is necessary to draw an arrow over each island such that any of those arrows is directed from α_i^- to α_i^+ . According to Remark 5, the directions of any two successive arrows will be opposite. Then one can continue the procedure recursively, drawing arrows of higher levels and identifying the position of h -strips with different indexes following to directions of the arrows. In simple terms, the order of h -strips of $(n+1)$ th level within an h -strip of n th level repeats the order of islands D_i , $i = -L, \dots, L$ within the set Δ_0 . The peculiarity is that the last index of embedded h -strips increases in direction from $\alpha_{i_0 \dots i_n}^-$ to $\alpha_{i_0 \dots i_n}^+$. An example of the ordering procedure is presented in Figure 5. As follows from the ordering procedure, the positions of h -strips with different indexes can be catalogued conveniently using a $(2L+1)$ -ary tree graph, where the root of the graph corresponds to the island D_0 and leaves of increasing levels denote h -strips with indexes of growing length. Figure 6 presents an example of such a tree for $L = 1$ (four levels of the tree are shown).

4. Algorithm for constructing of a gap soliton by the given code.

4.1. General remarks. Let $\hat{\psi}(x)$ be a gap soliton solution of (7). Then $\hat{\psi}(x)$ can be associated with an orbit $\mathbf{s} = \{\dots, p_{-1}, p_0, p_1, \dots\}$ whose entries are defined by $p_n = (\hat{\psi}(n\pi), \hat{\psi}_x(n\pi))$, $n \in \mathbb{Z}$. Since $\hat{\psi}(x)$ satisfies the localization condition (3), the orbit \mathbf{s} is a homoclinic loop of the fixed point $\mathcal{O}_0 = (0, 0)$, i.e., $\lim_{n \rightarrow \pm\infty} p_n = \mathcal{O}_0$. By the coding theorem, the orbit \mathbf{s} is associated with an unique code $a \in \Omega^N$ which has only a finite number of nonzero entries, i.e., it has the form

$$a = \{\dots, 0, 0, i_1, i_2, \dots, i_m, 0, 0, \dots\}, \quad i_1 \neq 0, \quad i_m \neq 0. \quad (18)$$

This code is naturally associated with the gap soliton $\hat{\psi}(x)$. By definition of Σ , the code (18) determines the order in which orbit \mathbf{s} visits the islands D_i , $i = -L, \dots, L$. Therefore this code can be obtained having the location of the islands and m coordinates of the points $(\hat{\psi}(n\pi), \hat{\psi}_x(n\pi))$, $n = 1, \dots, m$. This yields the answer to the Question 1 in Section 1.

Conversely, consider a code $a \in \Omega^N$ of the form (18). Due to Theorem 2.14, there exists an unique orbit \mathbf{s} which corresponds to this code, and according to Corollary 1 this orbit is a homoclinic loop of the fixed point $\mathcal{O}_0 = (0, 0)$. Let $p = (\psi_0, \psi'_0)$ be an arbitrary point of this orbit. Consider $\hat{\psi}(x)$, the solution of the Cauchy problem for (7) with the initial conditions

$$\hat{\psi}(0) = \psi_0, \quad \text{and} \quad \hat{\psi}_x(0) = \psi'_0. \quad (19)$$

TABLE 1. The relation between the entries of the code (18), the entries of the orbit $\mathbf{s} = \{\dots p_{-1}, p_0, p_1, \dots\}$ and the values of $\hat{\psi}(x)$ of (7), $i_1 \neq 0$, $i_m \neq 0$

Code a	\dots	0	\dots	0	i_1	\dots	i_m	0	\dots
Orbit \mathbf{s}	\dots	p_{-M}	\dots	p_0	p_1	\dots	p_m	p_{m+1}	\dots
Island	\dots	D_0	\dots	D_0	D_{i_1}	\dots	D_{i_m}	D_0	\dots
$\hat{\psi}(x)$	\dots	$\hat{\psi}(-M\pi)$	\dots	$\hat{\psi}(0)$	$\hat{\psi}(\pi)$	\dots	$\hat{\psi}(m\pi)$	$\hat{\psi}((m+1)\pi)$	\dots

This solution is a gap soliton, i.e., $\hat{\psi}(x) \rightarrow 0$ as $x \rightarrow \pm\infty$. Hence for construction of the profile of a gap soliton $\hat{\psi}(x)$ by the code (18) one has to find *any* entry of the orbit \mathbf{s} with sufficiently good accuracy. Then the profile of $\hat{\psi}(x)$ can be recovered from the numerical solution of the Cauchy problem (19).

4.2. Description of the algorithm. Consider a code of the form (18). Having infinite number of zeros from the left, this code corresponds to an orbit that remains in D_0 for infinitely many iterations of T^{-1} . The relation between the entries of the code (18), the entries of the orbit $\mathbf{s} = \{\dots p_{-1}, p_0, p_1, \dots\}$, $p_n = (\psi_n, \psi'_n)$, and the values of the solution $\hat{\psi}(x)$ of (7) is given in Table 1. Note that for $n \leq 0$ the points p_n are situated on \mathcal{V}_0 , the local unstable manifold of \mathcal{O}_0 , and for $n > m$ the points p_n lie on \mathcal{H}_0 , the local stable manifold of \mathcal{O}_0 .

Introduce the notation

$$(0 \times M) = \underbrace{00\dots 0}_{M \text{ times}}.$$

For instance, the h -strip indexed by M consecutive zeros and symbols $\{i_1, i_2, \dots, i_m\}$ is denoted by $H_{(0 \times M)i_1 \dots i_m}$. Since it is sufficient to find any entry of \mathbf{s} , we fix $M > 0$ (large enough) and seek for the entry p_{-M} . This entry can be characterized as follows:

(a) $p_{-M} \in H_{(0 \times M)i_1 \dots i_m(0 \times K)}$, where $K > 0$ is arbitrarily large, and

$$H_{(0 \times M)i_1 \dots i_m(0 \times K)} \subset \dots H_{(0 \times M)i_1 \dots i_m} \subset \dots H_{(0 \times M)i_1} \subset H_{(0 \times M)} \subset D_0; \quad (20)$$

(b) $p_{-M} \in \mathcal{V}_0$;

(c) $T^{M+m+1}p_{-M} \in \mathcal{H}_0$.

Let us take a closer look at the island D_0 . It is limited by a pair of h -curves α_0^+ and α_0^- and a pair of v -curves β_0^+ and β_0^- (see Figure 4). The curves α_0^\pm are such that if $q = (\psi, \psi') \in \alpha_0^\pm$, then the solution $\psi(x)$ of (7) with these initial data at $x = 0$ satisfies the condition $\lim_{x \rightarrow \pi} \psi(x) = \pm\infty$, (the sign $+$ or $-$ corresponds to the superscripts in α_0^\pm). According to Corollary 2, $T\mathcal{V}_0$ is an ∞ -curve that intersects α_0^+ and α_0^- , and $\mathcal{V}_0 = T\mathcal{V}_0 \cap D_0$. According to Definition 3.7, denote

$$h_0^- \equiv h_0^-(T\mathcal{V}_0) \equiv T\mathcal{V}_0 \cap \alpha_0^-, \quad h_0^+ \equiv h_0^+(T\mathcal{V}_0) \equiv T\mathcal{V}_0 \cap \alpha_0^+.$$

The points h_0^- and h_0^+ are rough bounds for the location of p_{-M} . Therefore p_{-M} is situated on $T\mathcal{V}_0$ between the points h_0^- and h_0^+ , see Figure 7.

Since $p_{-M} \in H_{0 \times M}$, consider h -strip $H_{0 \times M}$ in detail. This h -strip is bounded by two h -curves, $\alpha_{(0 \times M)}^-$ and $\alpha_{(0 \times M)}^+$, and each of them intersects $T\mathcal{V}_0$ in a unique point. Following Definition 3.8 denote these points by $h_{(0 \times M)}^-$ and $h_{(0 \times M)}^+$. The following relations hold

$$h_{0 \times M}^- = T^{-(M-1)}h_0^-, \quad h_{0 \times M}^+ = T^{-(M-1)}h_0^+$$

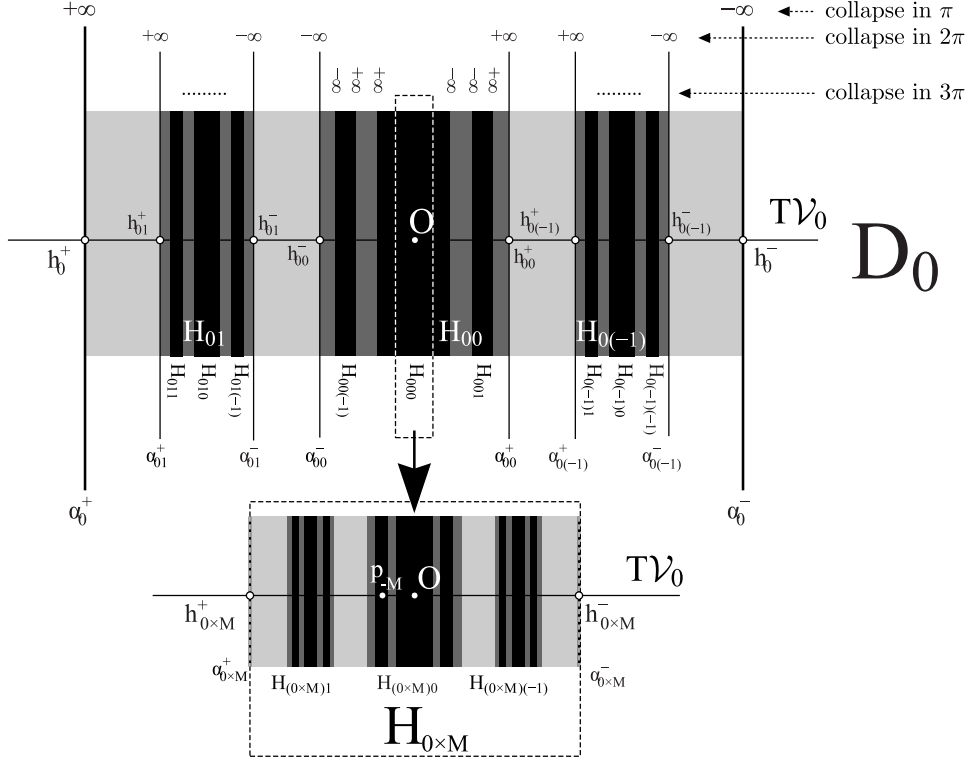


FIGURE 7. The scheme of the island D_0 , positions of h -strips and the points h_0^\pm , $h_{0i_1}^\pm$ for the case of coding using the alphabet of three symbols (the symbols are “-1”, “0” and “1”). The point p_{-M} is situated in the strip $H_{0 \times M}$ between the points $h_{0 \times M}^-$ and $h_{0 \times M}^+$.

The point p_{-M} is situated on TV_0 between the points $h_{0 \times M}^-$ and $h_{0 \times M}^+$.

Since the first nonzero symbol in the code (18) from the left is i_1 , the point p_{-M} is situated in h -strip $H_{(0 \times M)i_1} \subset H_{0 \times M}$. The strip $H_{(0 \times M)i_1}$ is bounded by two h -curves, $\alpha_{(0 \times M)i_1}^-$ and $\alpha_{(0 \times M)i_1}^+$, and each of them intersects TV_0 in a unique point. Denote these points by $h_{(0 \times M)i_1}^-$ and $h_{(0 \times M)i_1}^+$. The point p_{-M} is situated on TV_0 between the points $h_{(0 \times M)i_1}^-$ and $h_{(0 \times M)i_1}^+$.

Repeating this procedure following the chain (20), one concludes that p_{-M} is situated on TV_0 between the points $h_{(0 \times M)i_1 \dots i_m(0 \times K)}^-$ and $h_{(0 \times M)i_1 \dots i_m(0 \times K)}^+$. These points are the points of intersection of the boundary of $H_{(0 \times M)i_1 \dots i_m(0 \times K)}$ with TV_0 .

Finally, since the code (18) has infinite number of consecutive zeros from the right, $T^{M+m+K+1}p_{-M} \in \mathcal{H}_0$. Application of this condition completes the procedure.

4.3. Implementation. Let λ_1 be the eigenvalue of $DT(\mathcal{O}_0)$ such that $|\lambda_1| > 1$ and its corresponding normalized eigenvector be $e_1 = (\xi, \eta)$. Another eigenvalue of $DT(\mathcal{O}_0)$ is $\lambda_2 = 1/\lambda_1$, with corresponding normalized eigenvector $e_2 = (\xi, -\eta)$. The

vectors e_1 and e_2 are tangent to the local unstable \mathcal{V}_0 and local stable \mathcal{H}_0 manifolds in the point \mathcal{O}_0 correspondingly, see Remark 2. This means that if \mathbf{s} is a homoclinic orbit of \mathcal{O}_0 with components $p_n = (\psi_n, \psi'_n)$ then

$$\lim_{n \rightarrow +\infty} (\psi_n / \psi'_n) = -\xi / \eta, \quad \lim_{n \rightarrow -\infty} (\psi_n / \psi'_n) = \xi / \eta.$$

Let us introduce the parametrization on $T\mathcal{V}_0$ as follows: for $p \in T\mathcal{V}_0$ the value of parameter $\varepsilon = \varepsilon(p)$ is the length of the curve $T\mathcal{V}_0$ from the point \mathcal{O}_0 to the point p taken with the sign “+” if p lies between \mathcal{O}_0 and h_0^+ and the sign “−” if p is situated between \mathcal{O}_0 and h_0^- . The point p_{-M} is situated on the segment of $T\mathcal{V}_0$ between the points $h_{0 \times M}^-$ and $h_{0 \times M}^+$. For M large enough this segment is small and can be approximated by the tangent to \mathcal{V}_0 in \mathcal{O}_0 . Therefore, for homoclinic orbit of \mathcal{O}_0 with the code (18)

$$\psi_{-M} \approx \varepsilon \xi, \quad \psi'_{-M} \approx \varepsilon \eta, \quad |\varepsilon| \ll 1.$$

By the same reason, for K integer and large enough the following relation holds

$$\psi_{m+K} / \psi'_{m+K} \approx -\xi / \eta.$$

Once the parametrization is introduced, the numerical algorithm (see Algorithm 1) follows the steps of subsection 4.2. The main part of Algorithm 1 consists in consecutive finding of the bounds $\varepsilon(h_{(0 \times M)i_1}^-)$ and $\varepsilon(h_{(0 \times M)i_1}^+)$, $\varepsilon(h_{(0 \times M)i_1 i_2}^-)$ and $\varepsilon(h_{(0 \times M)i_1 i_2}^+)$, and so on. The algorithm exits with the value $\varepsilon^* = \varepsilon(p_{-M})$ found with a certain (controlled) accuracy. Once ε^* is found, then the shape of the soliton $\hat{\psi}(x)$ on the interval $x \in (-M\pi; K\pi)$ is described by the solution of Cauchy problem for (7) with initial data $\psi(-M\pi) = \varepsilon^* \xi$, $\psi_x(-M\pi) = \varepsilon^* \eta$. For $x < -M\pi$ and $x > K\pi$ the profile can be continued with linear asymptotics, i.e., by the solutions of (5) vanishing at $-\infty$ and $+\infty$, respectively, which are properly scaled to ensure the continuity of the whole solution and its derivative.

4.4. Some details. Algorithm 1 was implemented in Python using libraries `numpy` and `scipy`. It includes nested recursive procedure for processing of each index of the gap soliton code. The following details should be mentioned:

1. The Cauchy problem for (7) was solved using standard Runge-Kutta method of 4th order with constant step.
2. We found that the values $M = 2$ or 3 and $K = 2$ or 3 are enough for the most of the calculations. The accuracy was estimated by changing these parameters and comparing the results. In vicinity of the upper edge of the gaps (when the solitons are poorly localized) M and K should be increased.
3. The condition $\lim_{x \rightarrow n\pi} \psi(x) = \pm\infty$ that appears in the algorithm, was replaced by the condition $\psi(n\pi) = \psi_\infty$ where ψ_∞ is a large positive (or, correspondingly, great negative) number. Most of the calculations were fulfilled for $|\psi_\infty| = 10^6$ and checked for $|\psi_\infty| = 10^8$ to confirm that this choice of ψ_∞ does not affect the results.
4. The main difficulty in practical implementation of Algorithm 1 is caused by the fact that widths of h -strips $H_{(0 \times M)i_1 i_2 \dots}$ decrease rapidly as the number of indices grows. Therefore the difference

$$\left| \varepsilon(h_{(0 \times M)i_1 i_2 \dots}^+) - \varepsilon(h_{(0 \times M)i_1 i_2 \dots}^-) \right|$$

eventually becomes beyond the computer accuracy. This hinders the calculation of solitons with large m if the program code operates with floating-point numbers

with short mantissa. In order to overcome this difficulty, the `Python` library `gmpy2` for arbitrary-precision arithmetic was used. In principle, this allows to compute gap solitons with codes with arbitrary m (the algorithm was tested for codes with $m \leq 10$).

5. The algorithm does not allow to find gap solitons in the situation when Hypotheses 1–3 do not hold. In particular, it cannot be applied to compute small-amplitude gap solitons in cosine potential (6) with values (ω, A) situated close to the lower gap edges [see light-gray areas in (1)]. In this situation, a numerical continuation procedure in ω or in A can be applied.

5. Results. The algorithm was applied to (7) with cosine potential (6). Recall that according to Conjecture made in subsection 2.2, in Regions 1 and 2 on Figure 1 each gap soliton $\hat{\psi}(x)$ has a unique code of the form (18). For Region 1 the coding alphabet consists of 3 symbols, and for Region 2 it consists of 5 symbols. We denote the symbols of the alphabet by the integer numbers $-L, \dots, L$, where $L = 1$ for Region 1 and $L = 2$ for Region 2. This means that in Region 1 the coding alphabet is $\{-1, 0, 1\}$ and in Region 2 the coding alphabet is $\{-2, -1, 0, 1, 2\}$.

Let (18) be a code of a gap soliton. Let us call m the *length* of the code. In Region 1, the first band gap, there are 8 distinct gap solitons with codes of the length $m \leq 3$ (all other gap solitons with $m \leq 3$ can be obtained from them by involutions $x \rightarrow -x$ and $\psi \rightarrow -\psi$). Figure 8 presents the profiles of these gap solitons computed using Algorithm 1. The gap soliton in Figure 8(a) corresponds to the code $\{\dots, 0, 1, 0, \dots\}$. This solution is a fundamental gap soliton of the first gap (FGS₁) [24, 23] (in [22] this solution is called “on-site” gap soliton). FGS₁ is the unique elementary entity for Region 1. The code $\{\dots, 0, -1, 0, \dots\}$ corresponds to FGS₁ taken with minus sign (not shown in Figure 8). More complex gap solitons can be regarded as bound states of several FGS₁ taken with the plus or minus sign. For instance, the “off-site” gap soliton in the terminology of [22] has the code $\{\dots, 0, 1, -1, 0, \dots\}$ and can be regarded as a Figure 8(e).

In Region 2, inside the second band gap, there are 8 distinct (up to the involutions) gap solitons with codes of the length $m \leq 2$. Their profiles are shown in Figure 9. FGS₁ also presents as an elementary entity in Region 2 having the code $\{\dots, 0, 2, 0, \dots\}$ [see Figure 9(a)]. However there also exists another fundamental gap soliton FGS₂ with the code $\{\dots, 0, -1, 0, \dots\}$ [see Figure 9(e)]. This is the so-called *subfundamental* soliton which was introduced in [18]; solution of this type was also discussed in [23] where it was termed to as the second fundamental gap soliton. The code $\{\dots, 0, 1, 0, \dots\}$ corresponds to FGS₂ taken with minus sign. Again, more complex gap solitons can be regarded as bound states of FGS₁ and FGS₂ taken with different signs.

While the solitons illustrated in Figure 8 and Figure 9 correspond to relatively simple solutions with short codes ($m = 1, 2$ or 3), the algorithm is also applicable to more complex solitons and to solutions from higher gaps. For instance, in Figure 10 complex gap solitons, ($m = 10$) from the 2-nd and the 3-rd gaps are depicted.

6. Summary and discussion. In this paper we have proposed a numerical algorithm 1, for computation of localized modes for the spatially one-dimensional Gross-Pitaevskii equation with a periodic potential $U(x)$. These modes, i.e., gap solitons, are of the form $\Psi(x, t) = e^{-i\omega t}\psi(x)$ where $\psi(x)$ satisfies (7) and localization conditions (3). It is assumed that the parameters of the potential $U(x)$ allow

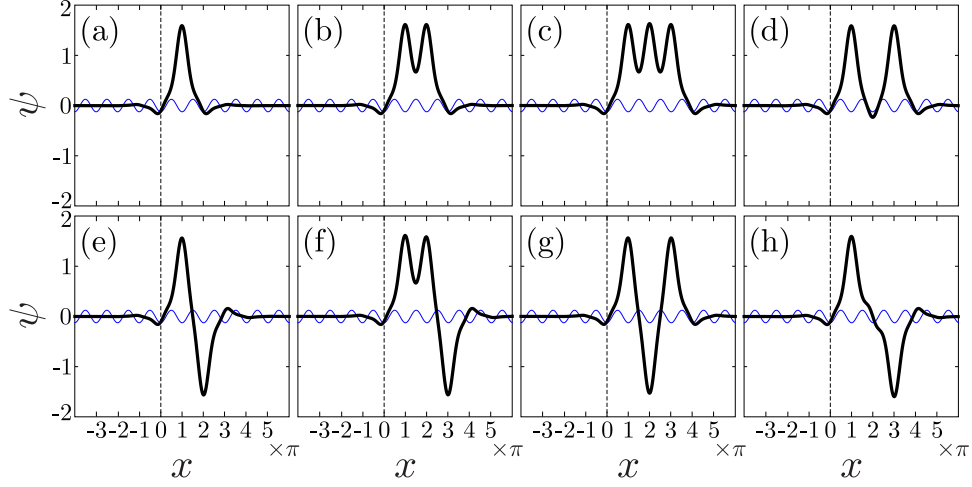


FIGURE 8. The gap solitons from Region 1, the first gap. Each panel shows the spatial profile of the soliton. The corresponding codes are: (a) $\{\dots, 0, 1, 0, \dots\}$; (b) $\{\dots, 0, 1, 1, 0, \dots\}$; (c) $\{\dots, 0, 1, 1, 1, 0, \dots\}$; (d) $\{\dots, 0, 1, 0, 1, 0, \dots\}$; (e) $\{\dots, 0, 1, -1, 0, \dots\}$; (f) $\{\dots, 0, 1, 1, -1, 0, \dots\}$; (g) $\{\dots, 0, 1, -1, 1, 0, \dots\}$; (h) $\{\dots, 0, 1, 0, -1, 0, \dots\}$. For all shown solutions $\omega = 1$ and $A = -3$. The vertical dashed line in each panel indicates the position of the point p_0 , such that $Tp_0 \notin D_0$, $T^{-n}p_0 \in D_0$, $n \geq 0$, see the explanation in subsection 4.2. Blue thin lines show schematically the cosine potential (6).

for coding of all these modes by bi-infinite sequences of symbols from some alphabet of finite length. It is known [3], that this coding is indeed possible, if certain assumptions (Hypotheses 1–3) hold, see Theorem 2.14. In particular, according to [3], the coding is possible for the potential $U(x) = A \cos 2x$, if the parameters ω (the frequency of the mode) and A (the amplitude of the potential) belong to vast areas on the plane (ω, A) , see Figure 1.

The coding approach exploits the fact that the “most” of solutions of (7) tend to infinity at some finite point of real axis. As a result the initial data for Cauchy problem for (7) corresponding to bounded in \mathbb{R} solutions form a fractal subset of \mathbb{R}^2 . The initial data corresponding to gap soliton solutions are situated in the intersection of this fractal set with the local unstable manifold \mathcal{V}_0 of the zero fixed point $\mathcal{O}_0 = (0, 0)$. The numerical procedure for computation of gap solitons consists in iterative localization of the segments on \mathcal{V}_0 where the initial data corresponding to a given code are situated. Then the profile of the nonlinear mode can be computed using the Runge-Kutta method. Algorithm 1 was implemented in `Python` and applied for gap solitons in cosine potential (6).

Algorithm 1 allows for various generalizations. With minor changes the algorithm can be applied in the case of more complex odd nonlinearities, both autonomous and non-autonomous. It is known that the structure of \mathcal{U}_π^\pm in (7) in cubic-quintic [6] and periodic [7] nonlinearities are similar to that described here, and therefore the application of Algorithm 1 in these cases is straightforward. For these problems, Algorithm 1 may be a useful tool to study bifurcations of gap solitons for (7) with

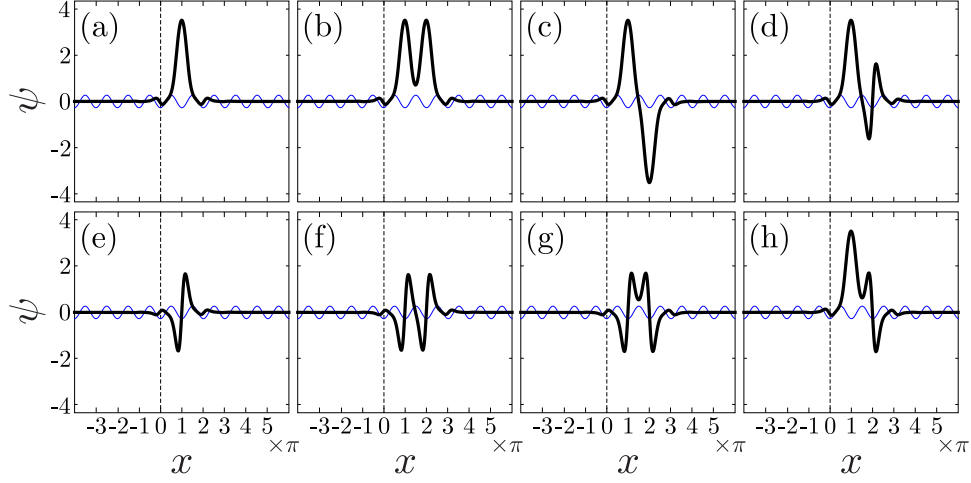


FIGURE 9. The gap solitons from Region 2, the second gap. The corresponding codes are: (a) $\{\dots, 0, 2, 0, \dots\}$; (b) $\{\dots, 0, 2, 2, 0, \dots\}$; (c) $\{\dots, 0, 2, -2, 0, \dots\}$; (d) $\{\dots, 0, 2, -1, 0, \dots\}$; (e) $\{\dots, 0, -1, 0, \dots\}$; (f) $\{\dots, 0, -1, -1, 0, \dots\}$; (g) $\{\dots, 0, -1, 1, 0, \dots\}$; (h) $\{\dots, 0, 2, 1, 0, \dots\}$. For all shown solutions $\omega = 4$, $A = -10$. The vertical line indicates the position of the point p_0 (see caption of Figure 8), and blue thin lines show schematically the cosine potential (6).

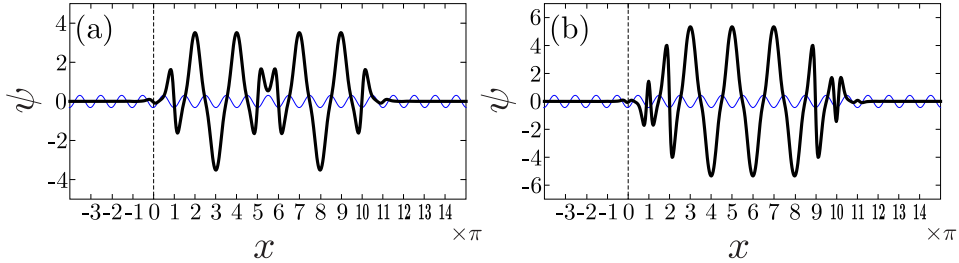


FIGURE 10. (a) Soliton from the second gap ($\omega = 4$, $A = -10$) with the code $\{\dots, 0, 1, 2, -2, 2, -1, 1, 2, -2, 2, -1, 0, \dots\}$. (b) Soliton from the third gap ($\omega = 10$, $A = -20$) with the code $\{\dots, 0, -1, 2, 3, -3, 3, -3, 3, -3, 2, 1, 0, \dots\}$. For each soliton the length of the code is $m = 10$.

different codes, similar to the one fulfilled in [4] for the intrinsic localized modes of the DNLS.

Another possible application of Algorithm 1 is the study of stability of gap solitons. An interesting question is whether it is possible to predict stability or instability of a gap soliton by its code. The results of this study will be reported elsewhere.

Appendix A. Proof of Theorem 3.1.

Proof. Consider the following nested intersections

$$\mathcal{V}_{i^*} \equiv V_{i^*i^*} \cap V_{i^*i^*i^*} \cap V_{i^*i^*i^*i^*} \cap \dots \quad (21)$$

$$\mathcal{H}_{i^*} \equiv H_{i^*i^*} \cap H_{i^*i^*i^*} \cap H_{i^*i^*i^*i^*} \cap \dots \quad (22)$$

Due to Lemma 3.1 from [3], the set \mathcal{V}_{i^*} is a v -curve and the set \mathcal{H}_{i^*} is an h -curve. An intersection of h -curve and v -curve, $\mathcal{V}_{i^*} \cap \mathcal{H}_{i^*}$, is a point which we denote by \mathcal{O}_{i^*} . Evidently, $T\mathcal{O}_{i^*}$ is a point having all its T -images and T -pre-images situated in D_{i^*} . Therefore $T\mathcal{O}_{i^*} \in \mathcal{V}_{i^*}$ and $T\mathcal{O}_{i^*} \in \mathcal{H}_{i^*}$, which implies that $T\mathcal{O}_{i^*} = \mathcal{O}_{i^*}$. Since the point of intersection of \mathcal{V}_{i^*} and \mathcal{H}_{i^*} is unique, \mathcal{O}_{i^*} is unique fixed point of T in D_{i^*} . The point (a) is proved.

Let us prove the point (b). According to the definition (21), $p \in \mathcal{V}_{i^*}$ if and only if $p \in D_{i^*}$ and $T^{-n}p \in D_{i^*}$ for any integer $n > 0$. This means that if $p \in \mathcal{V}_{i^*}$ then $T^{-1}p \in \mathcal{V}_{i^*}$, therefore \mathcal{V}_{i^*} is invariant with respect to action of T^{-1} . If $p \in \mathcal{V}_{i^*} \subset D_{i^*}$ then $T^{-1}p \in H_{i^*i^*} \subset D_{i^*}$, $T^{-2}p \in H_{i^*i^*i^*} \subset D_{i^*}$, etc. The h -strips $H_{i^*i^*}$, $H_{i^*i^*i^*}$, \dots form a nested sequence

$$\dots \subset H_{i^* \dots i^*} \subset \dots \subset H_{i^*i^*i^*} \subset H_{i^*i^*} \subset D_{i^*}$$

and the intersection in (22) is an h -curve which has the only one intersection point with \mathcal{V}_{i^*} at \mathcal{O}_{i^*} . This implies that if $p \in \mathcal{V}_{i^*}$ then the distance from \mathcal{O}_{i^*} to $T^{-n}p \in \mathcal{V}_{i^*} \cap H_{i^* \dots i^*}$ (n times i^*) can be made arbitrarily small by choosing n sufficiently large. Therefore the relation (15) is proved. The similar reasoning allows to prove (16). The point (b) is proved.

Finally, the orbit $\{\dots, p_{-1}, p_0, p_1, \dots\}$ corresponding to the code $\{\dots, i^*, i^*, i_1, i_2, \dots\}$, $i_1 \neq i^*$, has in D_{i^*} infinitely many successive entries p_k , $k < 0$. All of them are situated in all the strips $V_{i^*i^*}$, $V_{i^*i^*i^*}$, etc. Therefore, $p_k \in \mathcal{V}_{i^*}$, $k < 0$ and applying the reasoning of the point (b) one concludes that $\lim_{n \rightarrow \infty} p_{-n} = \mathcal{O}_{i^*}$. The point (c) is also proved. \square

Appendix B. The algorithm for computation of gap solitons.

REFERENCES

- [1] T. J. Alexander, E. A. Ostrovskaya and Yu. S. Kivshar, Self-Trapped Nonlinear Matter Waves in Periodic Potentials, *Phys. Rev. Lett.*, **96** (2006), 040401.
- [2] G. L. Alfimov, V. V. Konotop and M. Salerno, Matter solitons in Bose-Einstein Condensates with optical lattices, *Europhys. Lett.*, **58** (2002), 7–13.
- [3] G. L. Alfimov and A. I. Avramenko, Coding of nonlinear states for the Gross-Pitaevskii equation with periodic potential, *Physica D*, **254** (2013), 29–45.
- [4] G. L. Alfimov, V. A. Brazhnyi and V. V. Konotop, On classification of intrinsic localized modes for the discrete nonlinear Schrödinger equation, *Physica D*, **194** (2004), 127–150.
- [5] G. L. Alfimov, P. G. Kevrekidis, V. V. Konotop and M. Salerno, Wannier functions analysis of the nonlinear Schrödinger equation with a periodic potential, *Phys. Rev. E*, **66** (2002), 046608.
- [6] G. L. Alfimov and P. P. Kizin, On initial data for Cauchy problem for equation $u_{xx} + Q(x)u - P(u) = 0$ having no singularities on a given interval, *Ufa Mathematical Journal*, 2016, accepted.
- [7] G. L. Alfimov and M. E. Lebedev, On regular and singular solutions for equation $u_{xx} + Q(x)u + P(x)u^3 = 0$, *Ufa Mathematical Journal*, **7** (2015), 3–16.
- [8] V. I. Arnold, *Mathematical methods of classical mechanics*, Springer-Verlag, 1989.
- [9] I. V. Barashenkov, D. E. Pelinovsky and E. V. Zemlyanaya, Vibrations and Oscillatory Instabilities of Gap Solitons, *Phys. Rev. Lett.*, **80** (1998), 5117–5120.
- [10] I. V. Barashenkov and E. V. Zemlyanaya, Oscillatory instabilities of gap solitons: a numerical study, *Comp. Phys. Comm.*, **126** (2000), 22–27.
- [11] F. A. Berezin and M. A. Shubin, *The Shrödinger Equation*, Kluwer, Dordrech, 1991.

- [12] R. Fukuizumi and A. Sacchetti, Stationary States for Nonlinear Schrödinger Equations with Periodic Potentials, *J. Stat. Phys.*, **156** (2014), 707–738.
- [13] P. G. Kevrekidis, B. A. Malomed, D. J. Frantzeskakis, A. R. Bishop, H. Nistazakis and R. Carretero-González, Domain walls of single-component Bose-Einstein condensates in external potentials, *Mathematics and Computers in Simulation*, **69** (2005), 334–345.
- [14] P. P. Kizin, D. A. Zezyulin, G. L. Alfimov, Oscillatory instabilities of gap solitons in a repulsive Bose–Einstein condensate, *Physica D*, 2016, In Press.
- [15] V. V. Konotop and M. Salerno, Modulational instability in cigar-shaped Bose-Einstein condensates in optical lattices, *Phys. Rev. A*, **65** (2002), 021602.
- [16] P. J. Y. Louis, E. A. Ostrovskaya, C. M. Savage and Yu. S. Kivshar, Bose-Einstein condensates in optical lattices: Band-gap structure and solitons, *Phys. Rev. A*, **67** (2003), 013602.
- [17] B. A. Malomed and R. S. Tasgal, Vibration modes of a gap soliton in a nonlinear optical medium, *Phys. Rev. E*, **49** (1994), 5787.
- [18] T. Mayteevarunyoo and B. A. Malomed, Stability limits for gap solitons in a Bose-Einstein condensate trapped in a time-modulated optical lattice, *Phys. Rev. A*, **74** (2006), 033616.
- [19] D. E. Pelinovsky, A. A. Sukhorukov and Yu. S. Kivshar, Bifurcations and stability of gap solitons in periodic potentials, *Phys. Rev. E*, **70** (2004), 036618.
- [20] L. Pitaevskii and S. Stringari, *Bose–Einstein Condensation*, Clarendon Press, Oxford, 2003.
- [21] B. Wu and Q. Niu, Landau and dynamical instabilities of the superflow of Bose-Einstein condensates in optical lattices, *Phys. Rev. A*, **64** (2001), 061603(R).
- [22] J. Yang, *Nonlinear Waves in Integrable and Nonintegrable Systems*, SIAM, Philadelphia, 2010.
- [23] Yo. Zhang, Zh. Liang and B. Wu, Gap solitons and Bloch waves in nonlinear periodic systems, *Phys. Rev. A*, **80** (2009), 063815.
- [24] Yo. Zhang and B. Wu, Composition Relation between Gap Solitons and Bloch Waves in Nonlinear Periodic Systems, *Phys. Rev. Lett.*, **102** (2009), 093905.

Received xxxx 20xx; revised xxxx 20xx.

E-mail address: galfimov@yahoo.com

E-mail address: p.p.kizin@gmail.com

E-mail address: dzezyulin@fc.ul.pt

Algorithm 1 Computation of Gap Solitons

-
- 1: Fix M, K (integer, large enough).
 - 2: Compute the eigenvalues λ_1 and $\lambda_2 = 1/\lambda_1$, $|\lambda_1| > 1$, and corresponding eigenvectors, $e_1 = (\xi, \eta)$, $e_2 = (\xi, -\eta)$, of the fixed point \mathcal{O}_0 .
-

Phase 1: localization of the strip $H_{0 \times M}$

-
- 3: Solve numerically the Cauchy problem for (7),

$$x \in [0; M\pi], \quad \psi(0) = \varepsilon\xi, \quad \psi_x(0) = \varepsilon\eta,$$

for increasing values of ε spaced by small step $\Delta\varepsilon > 0$, from $\varepsilon = 0$, while $|\psi(M\pi)| < \infty$. Find $\varepsilon = \varepsilon^*$ corresponding to the conditions

$$|\psi(x)| < \infty, \quad x \in [0; M\pi) \quad \text{and} \quad \lim_{x \rightarrow M\pi} \psi(x) = \infty.$$

-
- 4: Assign $r := \varepsilon^*$ and $l := -\varepsilon^*$.
-

Phase 2: localization of the strips $H_{(0 \times M)i_1}, H_{(0 \times M)i_1 i_2}, \dots, H_{(0 \times M)i_1 \dots i_m}$

-
- 5: Allocate $A[0 : 4L + 1]$, an array of $4L + 2$ elements.

- 6: **for** $k = 1$ to m **do**

- 7: Solve numerically the Cauchy problem for (7),

$$x \in [0; (M + k - 1)\pi], \quad \psi(0) = r\xi, \quad \psi_x(0) = r\eta.$$

- 8: Assign $s := \text{sgn} \left\{ \lim_{x \rightarrow (M+k-1)\pi} \psi(x) \right\}$

- 9: Solve numerically the Cauchy problem for (7)

$$x \in [0; (M + k)\pi], \quad \psi(0) = \varepsilon\xi, \quad \psi_x(0) = \varepsilon\eta$$

for increasing values of ε , spaced by small step $\Delta\varepsilon > 0$, from $\varepsilon = l$ to $\varepsilon = r$ seeking for $4L + 2$ values $\varepsilon = \varepsilon_j^*$, $j = 0 \div (4L + 1)$, such that $\psi(x)$ satisfies the conditions

$$|\psi(x)| < \infty, \quad x \in [0; (M + k)\pi) \quad \text{and} \quad \lim_{x \rightarrow (M+k)\pi} \psi(x) = \infty.$$

Save the found $4L + 2$ values ε_j^* to the array $A[0 : 4L + 1]$ and sort A .

- 10: Assign $l := A[2L + 2si_k]$ and $r := A[2L + 2si_k + 1]$.

- 11: **end for**
-

Phase 3: localizing h -strips from $H_{(0 \times M)i_1 \dots i_m(0)}$ to $H_{(0 \times M)i_1 \dots i_m(0 \times K)}$

12: **for** $k = 1$ to K **do**

13: Solve numerically the Cauchy problem for (7)

$$x \in [0; (M + m + k)\pi], \quad \psi(0) = \varepsilon\xi, \quad \psi_x(0) = \varepsilon\eta$$

for increasing values of ε , spaced by small step $\Delta\varepsilon > 0$, from $\varepsilon = l$ to $\varepsilon = r$ seeking for $4L + 2$ values $\varepsilon = \varepsilon_j^*$, $j = 0 \div (4L + 1)$, such that $\psi(x)$ satisfies the conditions

$$|\psi(x)| < \infty, \quad x \in [0; (M + m + k)\pi] \quad \text{and} \quad \lim_{x \rightarrow (M+m+k)\pi} \psi(x) = \infty.$$

Save the found $4L + 2$ values ε_j^* to the array $A[0 : 4L + 1]$ and sort A .

14: Assign $l := A[2L]$ and $r := A[2L + 1]$.

15: **end for**

Phase 4: matching with asymptotics at $x \rightarrow +\infty$

16: Solve numerically the Cauchy problem for (7)

$$x \in [0; (M + m + K)\pi], \quad \psi(0) = \varepsilon\xi, \quad \psi_x(0) = \varepsilon\eta$$

for increasing values of ε , spaced by small step $\Delta\varepsilon > 0$, until finding $\varepsilon = \varepsilon^*$ such that $\psi(x)$ satisfies the condition

$$\frac{\psi_x((M + m + K)\pi)}{\psi((M + m + K)\pi)} = -\frac{\eta}{\xi}$$
